DIVISÃO 1 - SOLO NO ESPAÇO E NO TEMPO

Comissão 1.1 – Gênese e morfologia do solo

Nota

INTERNAL STRUCTURE OF A VERMICULAR IRONSTONE AS DETERMINED BY X-RAY COMPUTED TOMOGRAPHY SCANNING

Yuri Lopes Zinn[1]*, Carla Eloize Carducci[2] and Marla Alessandra Araujo[3]

[1] Universidade Federal de Lavras, Departamento de Ciência do Solo, Lavras, Minas Gerais, Brasil.
[2] Universidade Federal de Santa Catarina, Departamento de Agronomia, Curitibanos, Santa Catarina, Brasil.
[3] Universidade Federal de Lavras, Programa de Pós-graduação em Ciência do Solo, Lavras, Minas Gerais, Brasil.
* Corresponding author.
  E-mail: ylzinn@dcs.ufla.br

ABSTRACT

Ironstones or petroplinthites are common materials in soils under humid tropical climate, generally defined as the result of Fe oxide accumulation in areas where the water table oscillates, and may exhibit considerable morphological variability. The aim of this study was to examine the internal structure and porosity of an ironstone fragment from a Petroferric Acrudox in Minas Gerais, Brazil, by computed tomography (CT) and conventional techniques. The sample analyzed had total porosity of 59.5 %, with large macropores in the form of tubular channels and irregular vughs, the latter with variable degrees of infilling by material released from the ironstone walls or the soil matrix. The CT scan also showed that the ironstone has wide variation in the density of the solid phase, most likely due to higher concentrations or thick intergrowths of hematite and magnetite/maghemite, especially in its outer rims. The implications of these results for water retention and soil formation in ironstone environments are briefly discussed.

Keywords: laterite, soils with plinthite, density, mineralogy.

RESUMO: *ESTRUTURA INTERNA DE UMA PETROPLINTITA VERMICULAR ANALISADA POR TOMOGRAFIA COMPUTADORIZADA DE RAIOS-X*

Petroplintitas são materiais comuns em solos sob clima tropical úmido, geralmente definidas como resultado do acúmulo de óxidos de Fe em ambientes de oscilação freática, e podem apresentar considerável diversidade morfológica. Este trabalho visou estudar fragmentos de petroplintita extraídos de um Plintossolo Pétrico concrecionário de Minas Gerais, por meio de tomografia computadorizada e técnicas convencionais. Observou-se que a amostra de petroplintita analisada apresentou porosidade total de 59,5 %, com grandes poros na forma de canais tubulares e cavidades irregulares, estes últimos com graus diferentes de preenchimento por material desprendido das paredes da petroplintita ou do solo circunvizinho. A tomografia evidenciou também que a petroplintita estudada apresentou grande variação em densidade da sua fase sólida, provavelmente refletindo maiores concentrações ou intercrescimentos de hematita, maghemita ou magnetita, especialmente em suas partes mais externas. São brevemente discutidas as implicações desses resultados para a retenção de água e pedogênese nos ambientes de ocorrência das petroplintitas.

Palavras-chave: laterita, Plintossolo Pétrico, densidade, mineralogia.

INTRODUCTION

The Brazilian Soil Classification System defines *petroplinthite* as a material often derived from plinthite, which through repeated cycles of wetting and drying becomes vigorously cemented, forming ferruginous nodules or concretions (ironstones, lateritic concretions, *canga*, etc.) of variable size and shape (laminar, nodular, spherical, or oblong, in a vertical or irregular position), either isolated or forming a continuous layer (Embrapa, 2006). Such definition is similar to that of ironstone in Soil Taxonomy (Soil Survey Staff, 2010). In accord to the definition of laterites by Stoops and Marcelino (2010), ironstones can be understood as highly weathered soil materials, rich in hydrated oxides of Fe and Al, formed by their residual or absolute accumulation through dissolution, movement, and precipitation of Al, Fe, and Mn. The occurrence of ironstones in soils is generally deemed unfavorable for agricultural purposes, since they pose a hindrance to site mechanization, but also for their inherently low nutrient contents. However, ironstones have been used for millennia as raw material for road beds or building materials, and show potential for use as a sorbent for toxic substances.

The morphological and genetic diversity of ironstones and laterites is such that even the more accepted attempts to classify or describe a "typical" profile have been subject to severe criticism (Bourmann and Ollier, 2002), mostly because of the necessary simplification. Nonetheless, some basic ironstone types are recognized. In Soil Taxonomy (Soil Survey Staff, 2010), these materials often have irregular inclusions of clays, mostly of a tubular shape, which can be removed by water flow, leaving coarse channel voids. Stoops and Marcelino (2010) call this ironstone "vermicular laterite", in contrast to "nodular laterite". Theoretically, vermicular laterites or ironstones comprise a complex network of coarse and connected pores able to store water

available to plants. The study of ironstones poses considerable practical difficulty, not only in sampling this cemented material which is in fact a sedimentary rock formed in soil environments, but also through the extensive presence of opaque (Figure 1) and amorphous compounds, which complicate microscopic and mineralogical analyses (Stoops and Marcelino, 2010). Within a rationale of enhancing current understanding of ironstones, this study aimed to examine the internal structure and porosity of an ironstone fragment from a Petroferric Acrudox in Minas Gerais, Brazil, by computed tomography (CT) and conventional techniques.
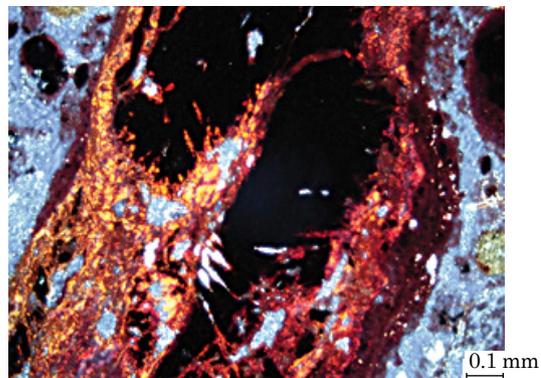
MATERIAL AND METHODS

Ironstone samples of around 10 cm length were collected from an apparently continuous but dismantling layer from the B horizon of a Petroferric Acrudox (Plintossolo Pétrico concrecionário) near Bom Sucesso, Minas Gerais, Brazil. This soil developed from alteration of serpentinite in the middle tier of the landscape, and it is marked by high particle density (3.8 kg dm^{-3}) resulting from the predominance of hematite (~72 % Fe$_2$O$_3$), occurrence of magnetite/maghemite, and the absence of kaolinite. Morphologically, this soil is characterized by abundant ironstone (48 % of the B horizon), sandy texture (hematitic sand), and fine granular structure, as well as very high phosphate sorption and excess exchangeable Mg^{2+} in comparison to Ca^{2+} (Araujo et al., 2014). An undisturbed soil sample was taken from the A horizon, oven-dried, and impregnated with an epoxy resin for thin section preparation and micromorphological description. Bulk density (ρ_b) of an ironstone sample (Figure 2) was determined by the principle of Archimedes, i.e., through immersion of an oven-dried, PVC-coated sample in distilled, degassed water, simulating the paraffin method for soil clods (Grossman and

Reinsch, 2002). The particle density (ρ_p) of the same sample, ground <2 mm, was then determined by the pycnometer method (Flint and Flint, 2002). Total porosity was then calculated by the formula $100(\rho_p - \rho_b)/\rho_p$. Ironstone samples were also finely ground with mortar and pestle for total C and N analyses by dry combustion (Nelson and Sommers, 1996) in a Vario MAX CN device (Elementar Americas, Hanau, Germany).
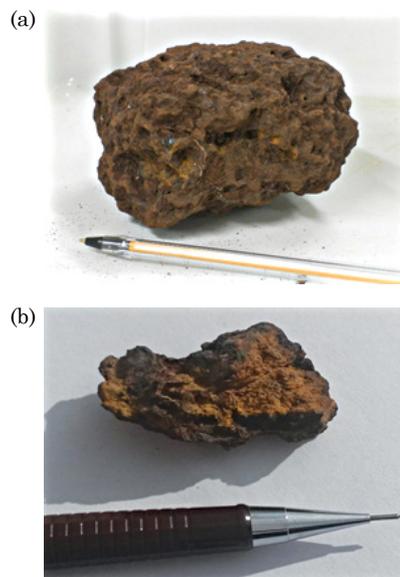
For computed tomography (CT) analysis, another ironstone sample was scanned by a cone of X-rays emitted by a tungsten target, working at 120 kV and 170 mA, in a 3rd generation, pre-clinical *microCT scan* (EVS/GE MS8x-130), generating a two-dimensional image of X-ray attenuation every 3.5 s. Since the X-rays thus generated were polychromatic (Clausnitzer and Hopmans, 2000), a 0.5 mm thick Cu filter of high transparency was used to avoid artifacts and maximize contrast between the solid and gaseous phases of the sample. The 2-D images were generated with a 20 µm spatial resolution, resolved at 70 µm, and recorded with radiometric resolution of 16 bits. Final image reconstruction was performed with the Explore Reconstruction Utility (GE Healthcare, 2006) software, with isovolumetric spatial resolution of 70 µm, resulting in individual volumes of 0.1269 mm^3 (700 voxel *vs* 700 voxel *vs* 370 images). Then, a Gaussian filter (radius=1) was used to reduce noise and artifacts, with the MicroView (GE Healthcare, 2006) software. In short, each of the 370 image planes of 700 × 700 voxels is composed of 490,000 voxels, for a total of 181,300,000 voxels. The length and thickness of selected features were measured with software tools for better sample characterization.

RESULTS AND DISCUSSION

Ironstone bulk and particle density analyses returned values of 1.37 e 3.38 kg dm^{-3}, respectively. Bulk density was not particularly high in comparison to common soils, whereas particle density of the ironstone was lower than the 3.8 kg dm^{-3} reported for this soil (Araujo et al., 2014). Since this ironstone had total C and N concentrations of 2.8 and 0.1 g kg^{-1}, respectively, and these values were much lower than those of bulk soil, it is unlikely that the relatively low particle density of ironstone was due to high organic matter levels. Thus, the low particle density of this ironstone can be ascribed to a higher occurrence of quartz in comparison to the soil, as well as the advanced stage of weathering, shown by visible dismantling and hydration of the concretionary material (Figures 1 and 2). The density data for this ironstone allow an estimate of total porosity of around 59.5 %, similar to values commonly reported for Oxisols.
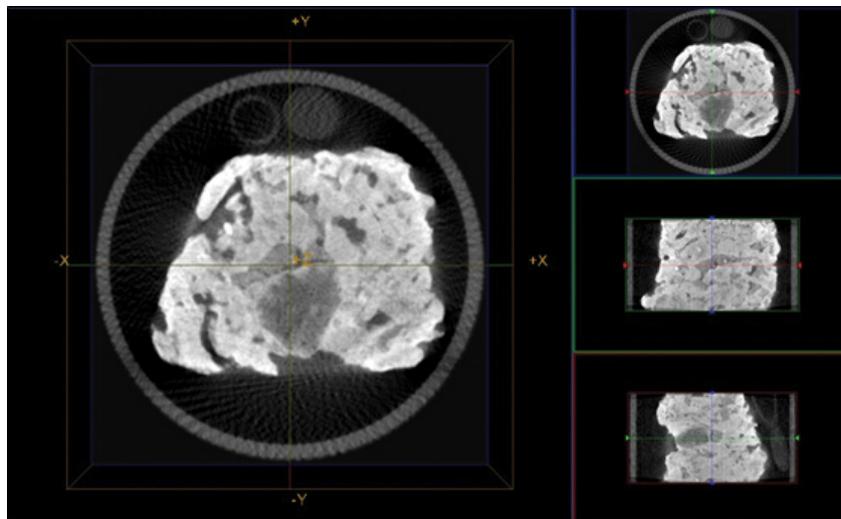

Figure 1. Thin section of the A horizon of the Petroferric Acrudox, showing the opaque cores of a dismantling ironstone, surrounded by a partially deferrified matrix (bright red and orange masses). The fragment appears to disintegrate, creating a friable outer rim of brown colors, which seems to give rise to the microgranular peds within the packing voids (blue colors). Image taken between partly crossed polarizers.

Figure 2. (a) Natural fragment of ironstone used for bulk and particle density determination (note root remains on the surface); (b) ironstone fragment showing a black color due to predominance of macrocystalline Fe oxides, and yellowish masses suggesting oxide hydration and disintegration.

The CT scan (Figure 3) showed two essential characteristics of this ironstone: 1) the existence of large, internal voids/pores, and 2) detectable differences in particle density. In regard to pore volume, there is marked occurrence of elongated pores, apparently tubular in shape ("vermicular")

Figure 3. Cross-section of an ironstone fragment (47 × 38 mm, in the XY axis) showing "vermicular" porosity, large irregular partially infilled pores, and dense masses (bright areas) on the outer rims or isolated grains. The large image shows the combination of the X, Y, and Z (Z orthogonal to XY) axes. The smaller images show, from top to bottom, the XY, XZ, and ZY planes.

at the left side of the main image in figure 3, reaching around 12 mm in length and 1.5 mm in diameter. A large pore of around 15 × 14 mm is visible at the core of the sample, as well as many other smaller, irregular pores. This feature of large inner macroporosity fits well with the calculated total porosity, suggesting that these ironstones can store water in flooded subsoils. However, not all large macropores in the sample are similar, since there are widely different amounts of loose infilling materials within them. For instance, in figure 3, the black color of the vermicular pores mentioned above is comparable to that surrounding the sample, demonstrating that these pores are effectively void, i.e. without any infillings by loose materials. Conversely, the large pore discussed above and other surrounding pores show different tones of gray (Figure 3), suggesting the presence of variable degrees of infilling by loose materials. According to Stoops and Marcelino (2010), materials filling in the vermicular pores are generally of a microgranular structure, due to removal of Fe from ironstone fragments, which essentially become loose soil material (Figure 2). This process can also be seen in figure 1, in which microgranular peds occupy the packing voids surrounding an ironstone fragment.

The rather unequal mass distribution within the ironstone is not only due to differences in macroporosity. Considerable portions of the solid phase appear in figure 3 with bright tones of white, due to the presence of materials with high particle densities. Such dense matter occurs more frequently on the outer rims of the sample, and as isolated grains up to a 2 mm diameter. Although a CT scan does not allow determination of the composition of this denser matter, it is likely that the continuous white areas comprise large domains or intergrowths of hematite, maghemite, or magnetite. Such minerals have particle densities from 4.9 to 5.3 kg dm^{-3}, much higher than the quartz and gibbsite which are also part of the mineral suite of this soil (Araujo et al., 2014). The fact that these dense materials occur chiefly at the surface of the sample suggests the intense effect of wetting/drying cycles, or even wildfires, favoring the secondary genesis of hematite, maghemite, or thermal reduction to magnetite (Viana et al., 2006). Possibly, the milimetric, dense grains are chiefly composed of the same Fe oxides. Areas with less bright tones of gray are composed of the same minerals, but probably with lower frequency of Fe oxide intergrowths, such that less dense minerals (quartz, amorphous phases, gibbsite) become predominant.

CONCLUSIONS

The ironstone studied showed large macroporosity, both as vermicular channels and irregular vughs.

Such macropores presented variable degrees of infilling by materials coming from disintegration of the ironstone itself, or from the soil matrix, which is probably a characteristic common to most vermicular ironstones.

The presence of denser masses in the solid phase is probably due to higher concentrations of macrocrystalline Fe oxides, especially on its outer surfaces.

The computed tomography scan proved a valuable method for study of ironstones, and can present new perspectives if used for ironstones of different chemical and mineralogical compositions, formed in other soil environments.

ACKNOWLEDGMENTS

REFERENCES

Araujo MA, Pedroso AV, Amaral DC, Zinn YL. Paragênese mineral de solos desenvolvidos de diferentes litologias na região sul de Minas Gerais. R Bras Ci Solo. 2014;38:11-25.

Bourmann RP, Ollier CD. A critique of the Schellmann definition and classification of 'laterite'. Catena. 2002;47:117-31

Clausnitzer V, Hopmans JW. Pore-scale measurements of solute breakthrough using microfocus X-ray computed tomography. Water Resour. Res. 2000;36:2067-79.

Empresa Brasileira de Pesquisa Agropecuária - Embrapa. Sistema brasileiro de classificação de solos. Rio de Janeiro; 2006.

Flint AL, Flint LE. Particle density. In: Dane JH, Clarke Topp G, editors. Methods of soil analysis: Physical methods. Madison: Soil Science Society of America; 2002. Pt 4. p.229-40. (Book series, 5).

GE Healthcare Microview Analysis 2.2. Technical Publication. Direction 2407688. Revision 1 [internet]. 2006 [accessed Dec 12 2011]. Available: http://www.oucom.ohiou.edu/ou-microct.

Grossman RB, Reinsch TG. Bulk density and linear extensibility. In: Dane JH, Clarke Topp G, editors. Methods of soil analysis: Physical methods. Madison: Soil Science Society of America; 2002. Pt 4. p.201-28. (Book series, 5).

Nelson DW, Sommers LE. Total carbon, organic carbon, and organic matter: Laboratory methods. In: Sparks DL, editor. Methods of soil analysis: Chemical methods. Madison: Soil Science Society of America; 1996. Pt 3. p. 961-1010. (Book series, 5).

Soil Survey Staff. Keys to soil taxonomy. Washington: United State Department of Agriculture; 2010.

Stoops G, Marcelino V. Laterite and bauxitic materials. In: Stoops G, Marcelino V, Mees F, editors. Interpretation of micromorphological features of soils and regoliths. Amsterdam: Elsevier; 2010. p.329-50.

Viana JHM, Couceiro PRC, Pereira MC, Fabris JD, Fernandes Filho EI, Schaefer CEGR, Rechenberg HR, Abrahão WAP, Mantovani EC. Occurrence of magnetite in the sand fraction of an Oxisol in the Brazilian savanna ecosystem, developed from a magnetite-free lithology. Aust J Soil Res. 2006;44:71-83.